Journal of Visualization, Vol. 8, No. 4 (2005)347-355

Study on the Optimum Mixing Throat Length for Drive Nozzle Position of the Central Jet Pump

Prabkeao, C.*[1] and Aoki, K.*[2]

*1 Department of Mechanical Engineering, Faculty of Engineering, King Mongkuts Institute of Technology, Ladkrabang(KMITL), Bangkok, Thailand.
*2 Department of Mechanical Engineering, School of Engineering, Tokai University, Japan.

Received 28 February 2005
Revised 30 June 2005

Abstract : The present paper describes a numerical prediction of optimum mixing throat length for various drive nozzle positions of the central jet pump. The flow pattern and pressure distribution in the pump for various positions of the drive nozzle are investigated by three-dimensional numerical analysis using the RNG k-ε turbulent flow model. Numerical analysis was carried out for values of the nozzle throat ratio d/D of the jet pump of 0.5, 0.6 and 0.7, respectively. The static pressure in the flow field of the jet pump is calculated for the following conditions: (1) drive nozzle position from the entrance of the throat $l/D = 0 \sim 2.0$, (2) flow rate ratio $M = 0 \sim 1.2$, and (3) Reynolds number $Re = 3.6\times10^5$. These calculations revealed that (1) the optimum length of the mixing throat for $l/D = 0 \sim 1.0$ is $Lm/D = 2.0 \sim 3.5$, (2) the length of the mixing throat for $l/D = 0$ and $M = 0$ (suction flow rate ratio = 0) is approximately $Lm/D = 3.5$, and (3) the maximum efficiency is obtained for $d/D = 0.6$ at $l/D = 0.5$. Moreover, the flow pattern in the mixing throat is clarified through a spark tracing experiment. The results obtained in the visualization experiment and the numerically obtained mixing length agreed well.

Keywords : Jet pump, Mixing throat, Drive nozzle position, Mixing length.

1. Introduction

The jet pump is radically different from the centrifugal pump, since the jet pump contains no moving parts and has a much simpler structure. The jet pump transfers momentum from a high-velocity primary jet flow to a secondary flow, and is geometrically simple, consisting of only four main components, a nozzle, a suction chamber, a mixing throat, and a diffuser, as shown schematically in Fig. 1. The absence of moving mechanical parts eliminates the operational problems associated with bearings, seals, and lubrication, and jet pumps are often used under various special environments, because they have fewer mechanical problems compared to other pumps. In the jet pump, a high-pressure fluid (gas or liquid) passes through a nozzle as the motive flow. As the high-pressure fluid enters the nozzle, part of its potential energy (pressure) is converted into kinetic energy (velocity). This energy conversion leads to a drop in pressure downstream of the nozzle, where low-pressure fluid is sucked in through a chamber. The sudden drop in pressure in this chamber allows low-pressure fluid to be drawn in without being exposed to the full pressure of the motive stream or the downstream pipeline pressure. The high-pressure and low-pressure fluids then enter the mixing throat, where momentum and energy transfer takes place between the high-pressure and low-pressure fluids. The fluids then pass through a diffuser in which the diameter of the pipe

increases gradually and the velocity of the mixture is reduced. The reduction in the mixture velocity leads to the conversion of part of the kinematics energy to pressure, and further pressure recovery takes place.

The high-pressure and low-pressure fluids leave the jet pump at an intermediate pressure between the high and low pressures.

Therefore, the following factors are considered to affect the efficiency of the jet pump:

(1) Ratio d/D of the nozzle diameter d and the diameter D of the mixing throat.

(2) Distance l from the nozzle tip to the mixing throat entrance.

(3) Length L of the mixing throat.

It is necessary to clarify the relationship between the length L of the mixing throat and the distance l from the nozzle tip to the mixing throat entrance in order to determine the nozzle throat ratio d/D for optimum design of jet pump. The maximum efficiency has been reported to be approximately $d/D = 0.6$ (Cunningham and River, 1957; Mueller, 1964; Reddy and Kar, 1968; Sanger, 1970; Narui and Harada, 1979; Winoto et al., 2000).

However, the reported maximum efficiency of the jet pump differs according to each study, even for approximate values of the nozzle throat ratio d/D of 0.6. The position of the drive nozzle of the jet pump and the length of the mixing throat differed in these studies. Following results are reported on mixing throat length Lm of the jet pump by Oshima (1988), Ueda (1953) and Ichikawa (1952).

Oshima (1988) : $Lm = (12\sim13)\ D$ in $Re = 10^5\sim10^7$

Ueda (1953) : $Lm = (2\sim3)\ D$ in $l < 2D$

Ichikawa (1952) : $Lm = (2.5\sim4)\ D$ for the adequate nozzle position

As shown above, the mixing throat length Lm is different by the researcher. The relationship between performance and the mixing throat length and the nozzle position remains unclear. Until now, performance tests have not been conducted on the jet pump, and there have been few reports on the internal flow of the jet pump. Therefore, clarifying the relationship among the position of the drive nozzle, the mixing throat length and the flow pattern is important with respect to the jet pump performance. However, few reports have numerically analyzed the relationship between the internal flow and pump performance as the primary factors affecting the efficiency of the jet pump.

In the present study, the flow pattern and pressure distribution in the pump are investigated with respect to various values of the diameter ratio d/D and position l/D of the driving nozzle by three-dimensional numerical analysis using the RNG k-ε turbulent flow model. The relationship among the optimum position of the drive nozzle l/D, the nozzle diameter d/D, and the mixing length Lm/D is clarified based on these results. Moreover, the flow pattern in the mixing throat is clarified through visualization by using spark tracing method.

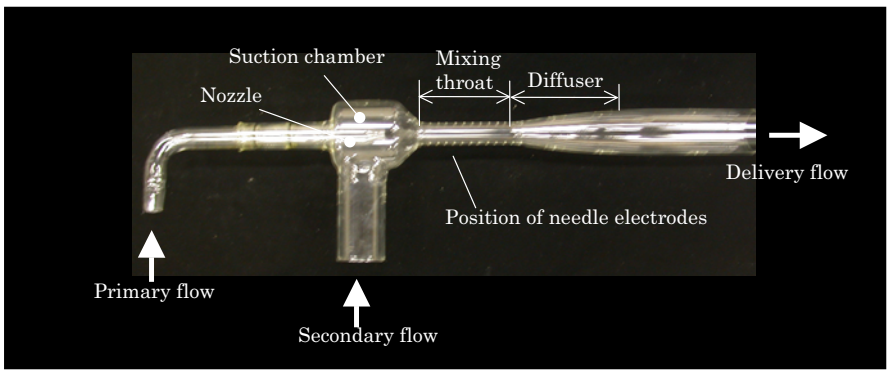

Fig. 1. Jet pump for visualization experiment made of the glass.

2. Experimental Apparatus and Method

2.1 Driving Fluid and Secondary Fluid Mixing in the Jet Pump Throat

The high-speed driving fluid flow and low-speed suction fluid flow mix in the throat division of the jet pump. Therefore, in order to improve pump efficiency, it is important to clarify the flow pattern in the mixing throat through a visualization experiment. Figure 1 shows the equipment used in the spark tracing visualization experiment. The test model is made of glass and consists of a nozzle, a suction chamber, a mixing throat and a diffuser.

The mixing throat has 10 needle electrode installation holes for visualizing the velocity distribution. For this visualization experiment the discharge voltage used was 125 kV, the pulsing frequency was 1000 Hz and number of pulses was 20.

2.2 Numerical Analysis

Figure 2 shows a schematic diagram of the central jet pump used in the present study. In the numerical analysis, the calculation of the static pressure and velocity distribution in the jet pump was carried out using the following parameters:

(1) Distance from the mixing throat entrance to the drive nozzle tip: $l/D = 0 \sim 2.0$.

(2) Flow rate ratio: $M = Q_s/Q_j$ (Q_s: secondary flow rate, Q_j: primary flow rate) = 0 ~ 1.2.

(3) Ratio of the nozzle diameter to the mixing throat diameter d/D: 0.5, 0.6 and 0.7.

(4) Flow velocity of the drive nozzle: $V_j = 30$ m/s.

(Here, the definition of Reynolds number $Re = V_j \times d / \nu = 360000$, ν: kinematic viscosity)

(5) For the structure shown in Fig. 3, grid number for the central jet pump: 45000 ~ 65000.
The analytical conditions are listed in Table 1.

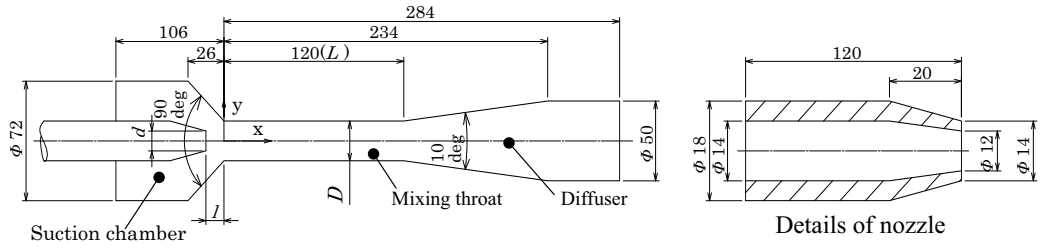

Fig. 2. Schematic drawings of the central jet pump.

Fig. 3. Meshes of the central jet pump.

Table. 1. Analytical condition.

Turbulent model		RNG k-e model
Grid		T-Grid
Calculation method		SIMPLE
Boundary condition	Wall	Wall law
	Entrance	Uniform flow
	Exit	Constant flow rate
Reynolds number (Velocity of nozzle)		360000 (V_j = 30 m/s.)
Number of Grid		45,000~65,000

3. Results and Discussion

3.1 Pressure and Velocity Distributions

Figures 4(a), (b), and (c) show the static pressure coefficient Cp for d/D = 0.5, 0.6, and 0.7, for the drive nozzle position of l/D = 0.5 ~ 2.0 and the flow rate ratio of M = 0.2. The static pressure coefficient, Cp, is defined as:

$$C_P = \frac{p - p_0}{\rho v_j^2 / 2} \tag{1}$$

where P is the static pressure in the throat and suction chamber, P_0 is the atmospheric pressure, ρ is the density, and v_j is the velocity of the drive nozzle.

The distribution of Cp in the suction chamber shows that the pressure is constant, regardless of either nozzle throat ratio d/D or nozzle position l/D, at atmospheric pressure.

However, the pressure gradually decreases with l/D, after reaching the maximum pressure value in the throat and the lowest pressure at the throat entrance.

The arrow in Fig 4 indicates the starting point of the constant negative pressure gradient after the static pressure reaches a maximum in the throat. This essentially indicates the mixing length Lm. The maximum pressure position moves to the downstream side as d/D decreases.

The pressure is minimum at the entrance of the throat and rapidly increases to reach the maximum value in the upstream portion of the throat. The pressure decreases due to the mixing loss as the flow moves downstream. Here, the pressure in the vicinity of the throat entrance is high when l/D is large. Moreover, the pressure drop increases according to the increase in the flow rate

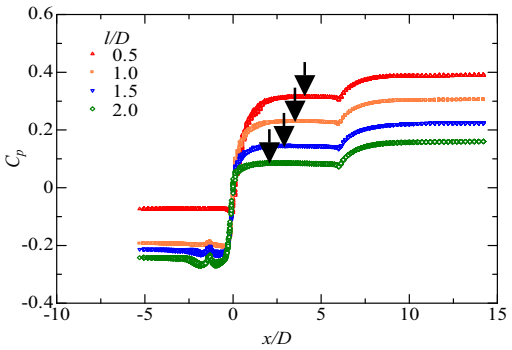

(a) d/D = 0.5

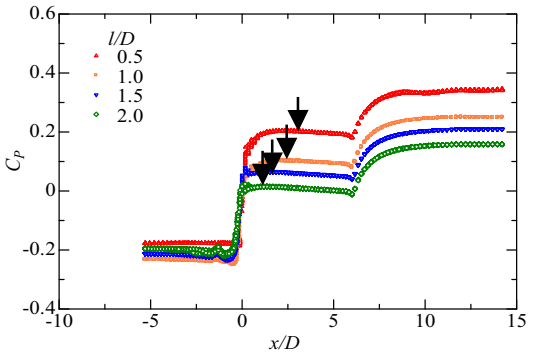

(b) d/D = 0.6

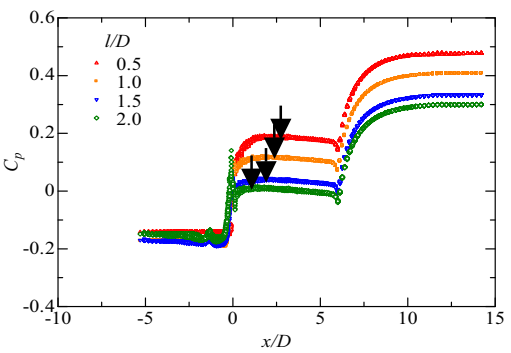

(c) d/D = 0.7

Fig. 4. Static pressure coefficient C_P in suction chamber and throat for various nozzle positions l/D for M = 0.2.

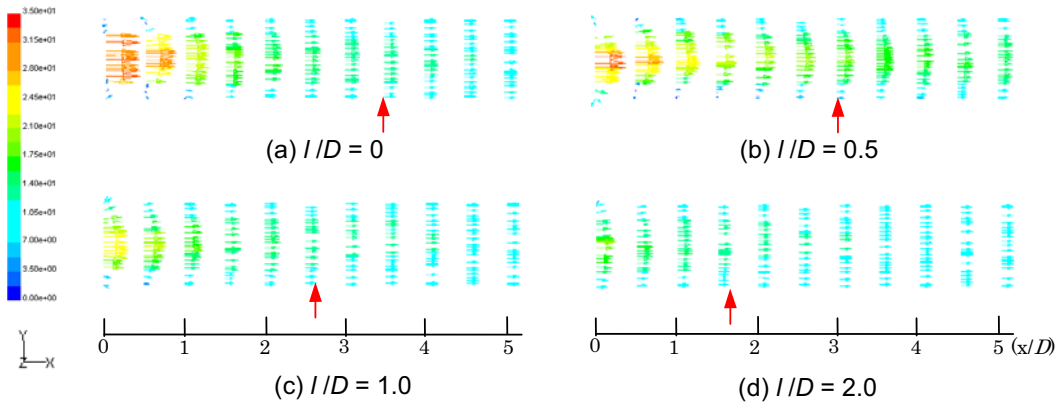

Fig. 5. Velocity vector colored by velocity magnitude for various nozzle positions *l* /*D* for *M* = 0.1.

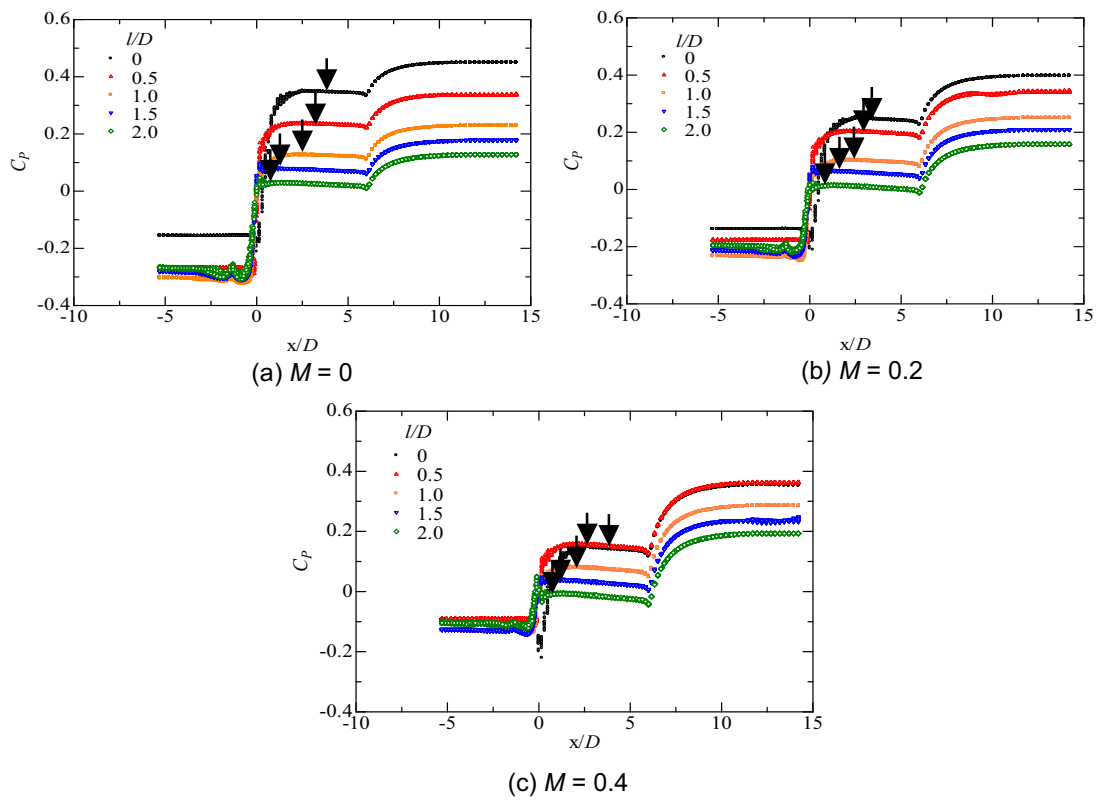

Fig. 6. Static pressure coefficient C_P in suction chamber and throat for various nozzle positions *l* /*D*.

ratio *M*. Here, the mixing length Lm is indicated by the distance from the position of the arrow to the throat entrance. That is to say, the mixing length Lm is defined as the smallest mixing length until the velocity distribution of the drive and suction flows reach becomes uniform in the throat.

The color arrow in Fig. 5 shows the velocity vector in the mixing throat for the nozzle position *l* /*D* = 0 ~ 2.0. Although the flow velocity of the throat entrance is uniform, when *l* /*D* is small, the circumferential flow velocity is reversed. The mixing length *Lm*/*D* at which the distribution of the flow velocity becomes uniform in the throat shifted downstream as the nozzle position becomes smaller. The arrow in the figure shows the position at which the flow distribution became uniform.

Figure 6 shows the variation of the static pressure coefficient with respect to the flow rate ratio $M = 0 \sim 0.4$ and nozzle position $l/D = 0 \sim 2.0$. The static pressure distribution decreases as the flow rate ratio M increases, and the static pressure decreases as l/D increases. The arrow in Fig. 6 shows the starting point of the constant negative pressure gradient for the static pressure, after reaching the maximum pressure in the throat.

3.2 Performance for the Nozzle Position

Figure 7 shows the relationship between Lm/D and l/D in the throat with respect to M for $d/D = 0.6$. The figure indicates that Lm/D becomes smaller as l/D increases, and Lm/D for a specific l/D becomes smaller with increasing M. These results indicate that the mixing length for the drive nozzle position is adequate for the following conditions:

1. $Lm/D = (2.0 \sim 3.5)$ for $0 \leq l/D \leq 1.0$
2. $Lm/D = (3.5)$ for $l/D = 0$ and $M = 0$

Figure 8 shows the relationship between the flow rate ratio M and the efficiency of the jet pump for various nozzle positions. The maximum efficiency is approximately 40% ($l/D = 0.5$ and $M = 0.6 \sim 0.7$) when the ratio of the nozzle diameter to the mixing throat diameter is 0.6. The pump efficiency shows an increasing tendency as the mixing length Lm/D increases with the nozzle position.

The efficiency η of the jet pump is defined as:

$$\eta = M \cdot N = \frac{Q_s}{Q_j} \cdot \frac{(P_d - P_s)}{(P_j - P_d)} \tag{2}$$

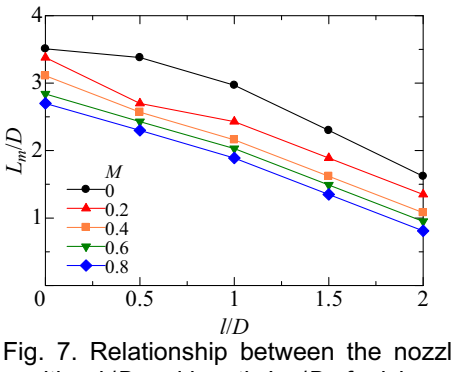

Fig. 7. Relationship between the nozzle position l/D and length Lm/D of mixing.

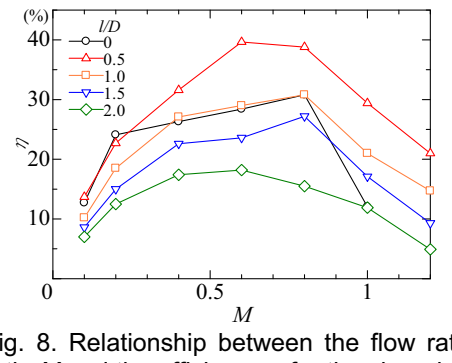

Fig. 8. Relationship between the flow rate ratio M and the efficiency η for the changing of the nozzle position l/D.

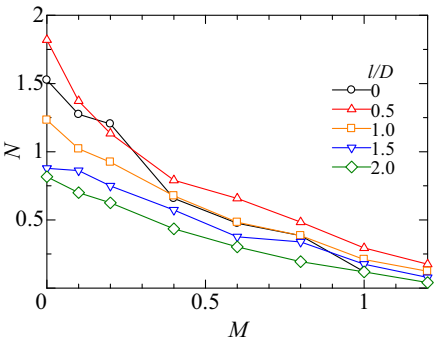

Fig. 9. Relationship between the flow rate ratio M and the head ratio N for different nozzle position l/D.

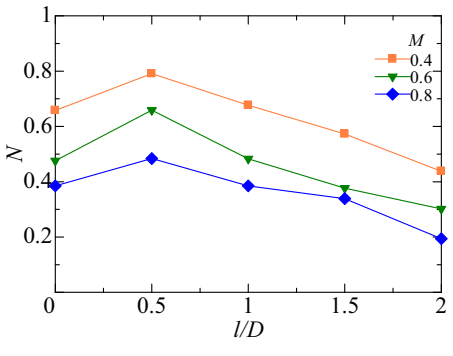

Fig. 10. Relationship between the nozzle position l/D and the head ratio N for different flow rate ratio M.

where M is the flow rate, N is the head ratio, P_j is the primary pressure, P_s is the suction pressure, and P_d is the delivery pressure.

Figure 9 shows the relationship between l/D and pressure head ratio N for the flow rate ratio M. For any value of M, the maximum pressure head ratio appears at $l/D = 0.5$. Figure 10 shows the relationship between the head ratio and the flow rate ratio M with respect to l/D. As the flow rate ratio increases, for either l/D, the head ratio N shows a decreasing tendency. However, the value of N is the greatest for the case of $l/D = 0.5$. That is to say, the efficiency $\eta = M \cdot N$ is high.

3.3 Visualization of Velocity Distribution in Mixing Throat Using Spark Tracing Method

These are various methods in the visualization of the jet (Kiwata et al., 2001; Fujisawa et al., 2004). Here, the flow visualization in jet pump mixer throat is tried using the spark tracing method.

The principle of the spark tracing method makes an instantaneous path of ionized air, when the electric spark travels in air. This path has a very low resistance for a very short period, during which detectable ionization exists. When a pair of electrodes is placed in the air flow to be measured and high-voltage pulses are applied to them, the first electric spark connects these electrodes through the shortest distance, making an ionized path. This ionized path moves together with the air flow, and the second electric spark travels along this moving path with very low electrical resistance. Subsequent electric sparks travel along the moving ionized path one after another, tracing the timelines of the air flow. Therefore, the movement of the ion is also disturbed, when the flow has been disturbed, and the velocity distribution in which the time line was also disturbed is shown.

Figure 11 shows the velocity distribution in the mixing throat as obtained by the spark tracing experiment, for drive nozzle positions l/D of 0.5 and 2.0 for $d/D = 0.5$, 0.6, and 0.7 and a flow rate ratio $M = 0.1$. From visualization result of the spark tracing method, it is possible to observe the reverse-directional flow in upstream wall surface of the mixing throat clearly. However, the flow can not be observed in the size of this figure, as it shifts to the downstream, since it decreases. Therefore, the decision of the position of the arrow was carried out from the enlarged view of the visualization result. It is known to decrease, as this reverse flow region goes to the downstream.

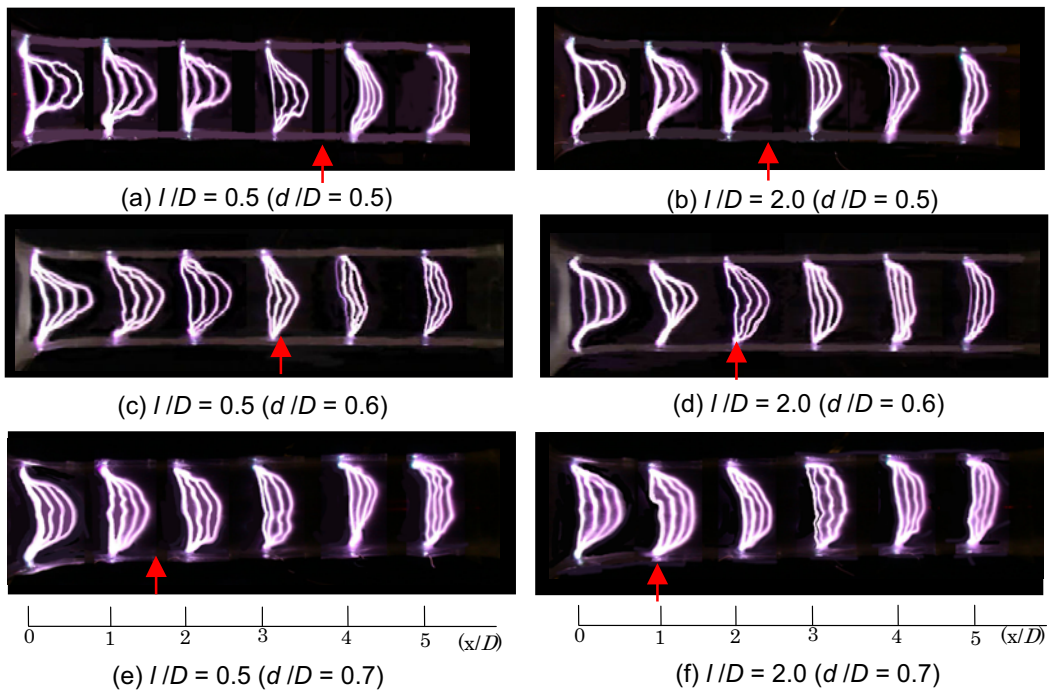

(a) $l/D = 0.5$ ($d/D = 0.5$) (b) $l/D = 2.0$ ($d/D = 0.5$)

(c) $l/D = 0.5$ ($d/D = 0.6$) (d) $l/D = 2.0$ ($d/D = 0.6$)

(e) $l/D = 0.5$ ($d/D = 0.7$) (f) $l/D = 2.0$ ($d/D = 0.7$)

Fig. 11. Visualization of velocity distributions in mixing throat by the spark tracing method for $M = 0.1$.

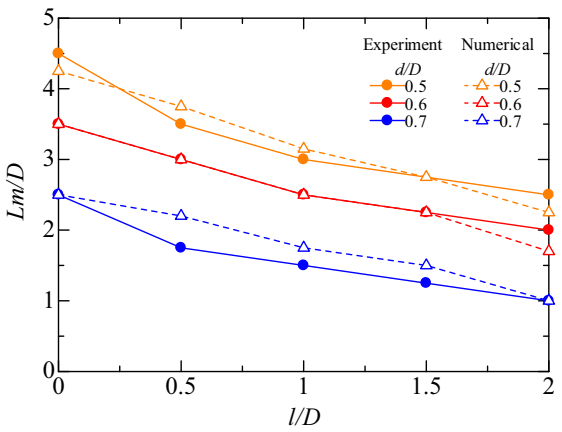

Fig. 12. Numerical and experimental results of the mixing length Lm/D for the change of the nozzle position l/D for M = 0.1.

The difference in the velocity distribution in the mixing throat can be understood from this visualization result. When l/D is small, the circumferential flow shows that reverse flow at the throat entrance is constant. Recirculation region near the wall in the mixing throat is moved downstream and the flow velocity becomes uniform. Here, the length at which the flow velocity in the mixing throat became uniform was defined as the mixing length. Therefore, the mixing length Lm/D is approximately 3.5 for l/D = 0.5. Moreover, Lm/D is approximately 1.5 for l/D = 2.0. As l/D increases, there is a tendency for the mixing length to move upstream. Moreover, the position at which the flow becomes uniform when d/D increases is found to move upstream. The arrow shown in the figure shows the position where the velocity distribution reached uniform flow velocity. Figure 12 compares the mixing length Lm/D obtained analytically from the velocity vector of Fig. 5 and the visualization results from Fig. 11. The length of the mixing throat Lm/D is indicated by the arrow. The mixing length obtained by the numerical analysis is in good agreement with the experimental results.

Mixing throat length for nozzle position is increased, as the flow ratio decreases in order to show in Fig 7. Therefore, it is important to study the relationship between mixing throat length for l/D in the smallest flow ratio. The results of Fig. 12 shows the relationship between mixing throat length as l/D are made to change to 0~2.0 at d/D = 0.5, 0.6 and 0.7. That is, for d/D = 0.5: Lm/D = 4.5~2.5, for d/D = 0.6: Lm/D = 3.5~1.75 and for d/D = 0.7: Lm/D = 2.5~1.0.

4. Conclusions

Numerical analysis and experimental evaluation for the optimum conditions of the length of the mixing throat in which the drive nozzle position and the diameter of the nozzle were varied revealed the following:

1. The static pressure coefficient increases as the nozzle position l/D decreases. Moreover, the length of the mixing throat Lm/D decreases as the throat diameter ratio d/D increases.

2. Mixing throat length Lm/D increases, as the flow ratio decreases, and as nozzle position l/D is closer to the mixing throat entrance. For the change of nozzle position l/D = 0~2.0, the optimum mixing throat length Lm/D for nozzle throat diameter ratio d/D = 0.5, 0.6 and 0.7 are as follows. Lm (2.5~4.5) D for d/D = 0.5, Lm = (2.0~3.5) D for d/D = 0.6 and Lm = (1.0 ~2.5) D for d/D = 0.7

3. The maximum efficiency was obtained for l/D = 0.5 and M = 0.6 ~ 0.7 for d/D = 0.6.

4. The variation in the velocity distribution in the mixing throat was clarified using the spark tracing method.

References

Cunningham, R. G. and River, W., Jet-pump theory and performance with fluid of high viscosity, Trans. ASME, 79 (1957), 1807-1820.
Fujisawa, N., Nakamura, K. and Srinivas, K., Interaction of Two Parallel Plane Jets of Different Velocities, Journal of Visualization, 7-2 (2004), 135-142.
Gosline, J. E. and O'Brien, M. P., The water jet pump, Univ. of Calif. Publ. In Engrg., 3-3 (1934), 167-190.
Ichikawa. T., Researches on the Jet Pump (1st Report) (Fluid: water, water), JSME, 18-69, (1951), 57-61.
Kiwata, T., Okajima, A. and Kimura, S., Flow Visualization of Vortex Structure of an Excited Coaxial Jet, Journal of Visualization, 4-1 (2001), 99-107.
Mueller, N. H. G., Water jet pump, J. Hyd. Div., ASCE, 90-3 (1964), 83-113.
Narui, H. and Harada, Y., A design method of water jet-water inducing pump, ASME Journal of Turbomachinery, 7-6 (1979), 377-383 (in Japanese).
Oshima, R., Studies on the Optimum Throat Length of Jet Pump, JSME, 54-497 (1988), 125-129.
Reddy, Y. R. and Kar, S., Theory and performance of water jet pump, Trans. ASCE J. Hyd. Div., 94-5 (1968), 1261-1281.
Sanger, N. L., An experimental investigation of several low -area-ratio water jet pump, ASME J. Basic Eng., 92-1 (1970), 11-20.
Ueda, T., Study on the Water Jet Water Pump, JSME, 20-89 (1954), 25-31.
Winoto, S. H., Li, H. and Shah., D. H., Efficiency of Jet Pumps, ASCE Journal of Hydraulic Engineering, (2000-9), 150-157.

Author Profile

Mr.Chamlong Prabkeao: He obtained his B.Sc. in Mechanical Engineering from King Mongkut's. Institute of Technology North Bangkok (KMITN), Thail in 1988 and M.Sc. in Mechanical Engineering from King Mongkut's. Institute of Technology Ladkrabang (KMITL), Bangkok, Thailand in 1996. He became an Associate Professor of Department of Mechanical Engineering, Faculty of Engineering, at KMITL in 1998. His area of expertise includes Hydraulic and Fluid Machinery. His current research interests cover jet pumps and their applications.

Katsumi Aoki: He received his M. Sc. (Eng.) degree in Mechanical Engineering in 1976 from Tokai University and his Ph. D. in Mechanical Engineering in 1986 from the same University. After obtaining M. Sc. he worked as a research assistant, a lecturer, and an associate professor at Tokai University before taking up his current position as a professor of Tokai University. His current research interest covers flow around a rotating circular cylinder with and without grooves, flow around a rotating sphere, possibility of drag reduction using triangle-type cavity and flow visualization by spark tracing method of complicated flow like in centrifugal blower.